Title

BRD4 is associated with raccoon polyomavirus genome and mediates viral gene transcription and maintenance of a stem cell state in neuroglial tumour cells.

Journal

The Journal of general virology, 97(11)

ISSN

0022-1317

Authors

Church, Molly E
Estrada, Marko
Leutenegger, Christian M
et al.

Publication Date

2016-11-01

DOI

10.1099/jgv.0.000594

Peer reviewed

Journal of General Virology (2016), **97**, 2939–2948 DOI 10.1099/jgv.0.000594

BRD4 is associated with raccoon polyomavirus genome and mediates viral gene transcription and maintenance of a stem cell state in neuroglial tumour cells

Molly E. Church,[1]† Marko Estrada,[2] Christian M. Leutenegger,[2] Florante N. Dela Cruz,[1] Patricia A. Pesavento[1] and Kevin D. Woolard[1]

[1]Department of Pathology, Microbiology and Immunology, School of Veterinary Medicine, University of California, Davis, CA, USA

[2]IDEXX Laboratories Inc, West Sacramento, CA, USA

Correspondence
Kevin D. Woolard
kdwoolard@ucdavis.edu

Polyomavirus infection often results in persistence of the viral genome with little or no virion production. However, infection of certain cell types can result in high viral gene transcription and either cytolysis or neoplastic transformation. While infection by polyomavirus is common in humans and many animals, major questions regarding viral persistence of most polyomaviruses remain unanswered. Specifically, identification of target cells for viral infection and the mechanisms polyomaviruses employ to maintain viral genomes within cells are important not only in ascribing causality to polyomaviruses in disease, but in understanding specific mechanisms by which they cause disease. Here, we characterize the cell of origin in raccoon polyomavirus (RacPyV)-associated neuroglial brain tumours as a neural stem cell. Moreover, we identify an association between the viral genome and the host cell bromodomain protein, BRD4, which is involved in numerous cellular functions, including cell cycle progression, differentiation of stem cells, tethering of persistent DNA viruses, and regulation of viral and host-cell gene transcription. We demonstrate that inhibition of BRD4 by the small molecule inhibitors (+)-JQ1 and IBET-151 (GSK1210151A) results in reduced RacPyV genome within cells *in vitro,* as well as significant reduction of viral gene transcripts LT and VP1, highlighting its importance in both maintenance of the viral genome and in driving oncogenic transformation by RacPyV. This work implicates BRD4 as a central protein involved in RacPyV neuroglial tumour cell proliferation and in the maintenance of a stem cell state.

Received 6 June 2016
Accepted 30 August 2016

INTRODUCTION

Polyomavirus infection in humans and other mammals is widespread and, in general, results in lifelong, persistent infections, rarely causing cytolytic or oncogenic disease (DeCaprio & Garcea, 2013; Moore & Chang, 2010). In a persistent viral infection, the viral genome is maintained within a cell over an extended period of time with little or no virion production. In contrast, a cytolytic (productive) infection produces abundant virions followed by lysis of the infected cell. Alternatively, infection by polyomavirus may result in neoplastic transformation, whereby oncogenic viral proteins promote constitutive cell division. Despite decades of research on polyomaviruses, major questions regarding viral persistence of most polyomaviruses remain unanswered, including identification of the target cells for persistence and the mechanisms polyomaviruses employ to maintain viral genomes within cells (DeCaprio & Garcea, 2013; Wirth *et al.*, 1997, 2013; Swanson *et al.*, 2009). In addition, interactions between viral and cellular proteins during the shift from a clinically silent, persistent infection to that of high virion production and cytolytic disease or neoplasia remain largely unknown (White *et al.*, 2013; Ferenczy *et al.*, 2013). Therefore, insights into the mechanisms utilized by polyomaviruses to regulate their genome during persistence and productive infection will further our understanding of not only viral tropism, but also the dynamic interplay between the host cell and viral genome. Ultimately identification of mechanisms governing viral persistence versus productive infection may identify novel mechanisms to prevent disease associated with viral infection.

†Present address: Department of Pathobiology, University of Pennsylvania School of Veterinary Medicine, Philadelphia, PA, USA.

Four supplementary figures and a supplementary table are available with the online Supplementary Material.

Raccoon polyomavirus (RacPyV) has been detected in every neuroglial tumour diagnosed in free-ranging raccoons in the western USA (CA, OR, WA) (Dela Cruz *et al.*, 2013). Despite the consistent anatomic site of these tumours in the olfactory tract, they have quite varied histological appearance and non-specific immunohistochemical profile, and prior studies have not identified a cell of origin (Giannitti *et al.*, 2014). The location of the olfactory tract, which is situated along the mammalian rostral migratory stream, a site rich in migrating neural stem cells, is of interest (Sun *et al.*, 2010). It has been suggested that Merkel cell carcinoma, a skin cancer in humans caused by the Merkel cell polyomavirus, arises after initial infection of stem cells in the skin (Tilling & Moll, 2012; Lemasson *et al.*, 2012). We therefore sought to investigate whether tumour cells shared characteristics specific to the stem cells in this unique anatomic site, and moreover, whether this stem cell state may be relevant to their capacity to be transformed by RacPyV. Mammalian neural stem cells are maintained through expression of transcription factors sox2 and olig2, and often co-express cytoplasmic filament proteins across multiple cell lineages, including neuron-specific class III beta-tubulin (TuJ-1), glial fibrillary acidic protein (GFAP), and A2B5, a membrane-associated protein present in glial lineages. In addition, there is a growing interest in the role of the chromosome-associated bromodomain protein, BRD4. This protein is implicated in numerous cellular functions, including maintenance of stem cells (Liu *et al.*, 2014; Rodriguez *et al.*, 2014; Wu *et al.*, 2015), regulation of the cell cycle (Josling *et al.*, 2012; Mochizuki *et al.*, 2008), tethering of persistent DNA viruses (Lin *et al.*, 2008; You *et al.*, 2004, 2006), and regulation of viral and host-cell gene transcription (McBride & Jang, 2013). Additionally, other investigators have identified BRD4 as a mediator of polyomaviral gene transcription and replication (Wollebo *et al.*, 2016). Given that these functions are applicable to questions of viral oncogenesis in general and overlap with questions regarding RacPyV specifically, we investigated the potential role BRD4 plays in RacPyV viral genome maintenance and in RacPyV-induced transformation. Here, we show that RacPyV-associated tumour cells grow in an analogous manner to neural stem cells, express numerous protein markers of stem cells, and express high levels of BRD4. Moreover, inhibition of BRD4 results in reduction of RacPyV genome, decreased expression of oncogenic viral proteins, decreased cell proliferation and loss of a stem cell state in these cells. We hypothesize that the cell of origin for these tumours is a neural stem cell and, furthermore, that expression of BRD4 specific to these neural stem cells is integral in maintenance of the RacPyV genome and transformation by this virus.

RESULTS

Tissue distribution of RacPyV

Determination of viral load in tissue was performed using a quantitative real-time PCR (qPCR) assay targeted to the VP1 region of the RacPyV genome. Genomic viral DNA was detected in multiple tissues including swabs of oropharyngeal and nasal mucosa, faeces, salivary gland, urine, brain, whiskers/skin, lymphoid tissue (tonsils and lymph nodes), kidney and tumour (Table 1). RacPyV DNA was identified in 100 % of brain tumours, as previously reported (Brostoff *et al.*, 2014), and among non-tumour tissues in raccoons both with and without brain tumours, the percentage of positive samples varied between 20 % (salivary gland) to 64 % (whiskers/skin). RacPyV was detected in significantly higher quantities in tumour tissue relative to any other tissue tested (Mann-Whitney test, $P<0.0001$). The viral DNA equivalents per mg of tumour tissue ranged from 3.4×10^5 up to 1.19×10^{11}, with a mean of 1.08×10^{10} (Fig. S1, available in the online Supplementary Material). In contrast, quantities were much lower in non-tumour tissues, ranging from 92 viral equivalents per mg faeces to 3.1×10^6 in brain tissue from raccoons without tumours and 1.5×10^{11} in brain tissue from raccoons with tumours.

Primary cell culture and characterization

To compare growth characteristics of cells from the tumour and potential sites of viral persistence, we initiated primary cell cultures from various tissues. We established cell lines from neuroglial brain tumours (Fig. 1a), neural stem cells isolated from the subventricular zone of physiologically normal raccoons (Fig. 1b), astrocytes from the cerebral cortex of physiological normal raccoons (Fig. 1c), fibroblasts from the dermis of physiologically normal raccoons (Fig. 1d), and tubular epithelium from kidney of physiologically normal raccoons (Fig. 1e). Both tumour cells and neural stem cells exhibit similar growth characteristics *in vitro*: both proliferate in serum-free, Neurobasal media and form non-adherent neurospheres, a characteristic of neural stem cells and neuroepithelial tumours in humans (Reynolds & Weiss, 1992; Ahmed, 2009) (Fig. 1a, b). In addition, raccoon tumour cell lines strongly express markers of stem cells including sox2, nestin, olig2 and A2B5 (Fig. 2a), and co-express markers of neuronal (TuJ-1) and glial (GFAP) cell lineages, indicating bipotential differentiation (Fig. 2a). In contrast, cortical astrocytes do not express sox2 or nestin (Fig. 2b) and only express GFAP (Fig. 2b). Cells isolated from the kidney express epithelial markers, including cytokeratins and the tight junction proteins, ZO-1 and occludin (Fig. 2c). Dermal fibroblasts expressed vimentin and were negative for markers of stem cells and epithelial cells, consistent with mesenchymal tissue (Figs 2c and S2).

In order to evaluate specificity of the antibodies used in raccoon primary cell immunofluorescence, we also performed an immunoblot using protein isolated from Rac14 tumour cells using the same antibodies. Renal tubular epithelium were used as negative controls (Fig. 2d).

In addition to immunocytochemistry, fluorescence-activated cell sorting was utilized to examine expression of neural stem cells by our tumour cells. A high percentage of Rac14 tumour cells express CD133 (approximately 28 %), with a small percentage co-expressing CD133 and CD15 (Fig. 3).

Table 1. Number of tissue samples analysed by quantitative PCR for RacPyV

	Tumour	Brain	Salivary gland	Kidney	Whiskers/ skin	Faeces	Oropharyngeal nasal swab	Urine	Lymphoid	Bone marrow
Total no. samples analysed	17	52	82	22	33	96	102	78	20	7
No. of minimally detectable samples (C_t<40)	17	2	7	4	12	15	17	10	4	2
Proportion minmally detectable	1.00	0.04	0.09	0.18	0.36	0.16	0.17	0.13	0.20	0.29
No. of positive samples (C_t<35)	17	17	9	1	9	11	14	7	1	0
Proportion positive	1.00	0.33	0.11	0.05	0.27	0.11	0.14	0.09	0.05	0.00
Total no. samples with RacPyV detected	17	19	16	5	21	26	31	17	5	2
Proporton of samples positive	1.00	0.37	0.20	0.23	0.64	0.27	0.30	0.22	0.25	0.29
Viral load (viral equivalents per mg or ml sample)										
Minimum	344 274	835	231	494	580	92.8	198	135	323	602
Maximum	1.19E+11	1.46E+11	123	10 034	2.13E+06	1.09E+06	4.39E+06	2.66E+06	14 453	2 421
Mean	1.08E+10	7.67E+09	96 951	2 825	162 843	48 647	232 357	233 182	413	1 512
SD	2.86E+10	3.34E+10	250 675	4 099	474 901	211 829	806 987	651 333	6 178	1 286

BRD4 expression and association with RacPyV

BRD4 was identified as a potential binding protein to RacPyV based on its role in other DNA viruses (McBride & Jang, 2013; Ottinger *et al.*, 2006; Wang *et al.*, 2012). We compared the expression of BRD4 across cell types by immunoblot, and identified high protein expression in the tumour cell line. BRD4 is also present in raccoon neural stem cells and to a lesser extent in the cells representing sites of persistence, the renal tubular epithelium (Fig. 4). BRD4 protein was not detected in dermal fibroblasts or cortical astrocytes.

In order to examine whether BRD4 is associated with the RacPyV genome, we performed chromatin immunoprecipitation (ChIP) using an antibody against BRD4, with PCR amplification of bound DNA directed against both the LT and VP1 regions of RacPyV. Our ChIP assay demonstrated that RacPyV is physically associated with BRD4 in cultured neuroglial tumour cells, as both early (LT) and late (VP1) RacPyV genes were amplified following immunoprecipitation with the BRD4 antibody (Fig. 5). Treatment of cells with (+)-JQ1 (hereafter referred to as JQ1), a BRD4 inhibitor that physically blocks the association with DNA confirmed the specificity of this association as it specifically reduced gene amplification of both LT and VP1 in BRD4-immunoprecipitated DNA compared to the histone H3 immunoprecipitation.

Decreased expression of stem cell markers with inhibition of BRD4

Following our identification of BRD4-associated RacPyV, we next investigated what functional roles inhibition of BRD4 would have in raccoon tumour cells. To explore the role BRD4 might play in maintenance of a stem cell state in tumour cells, we treated cells with small molecule inhibitors of BRD4 [JQ1 and IBET-151 (GSK1210151A)]. We then compared the cytomorphology and expression of neural stem cell markers or neuronal and glial differentiation markers against either vehicle control or the inactive enantiomer (−)-JQ1. Immunocytochemistry demonstrated that inhibition of BRD4 abrogates expression of neural stem cell markers, as well as increasing expression of both TuJ-1 and GFAP, implying increased differentiation. (Figs 6 and S3).

Effect of BRD4 inhibition on growth kinetics in RacPyV-infected tumour cells

In order to assess whether the decrease in neural stem cell markers and increase in differentiation coincides with decreased proliferation, we analysed cell viability and proliferation by MTT assay and flow cytometry, respectively. The MTT assay reveals a significant reduction in the average absorbance of tumour cells treated with JQ1 (0.062) compared with control cells (P<0.0001, unpaired t-test), indicating that BRD4 inhibition decreases cell viability and proliferation.

To examine the effect of BRD4 inhibition on cell proliferation, we examined EdU-incorporation into actively dividing cells by flow cytometry. Cell cycle analysis revealed a

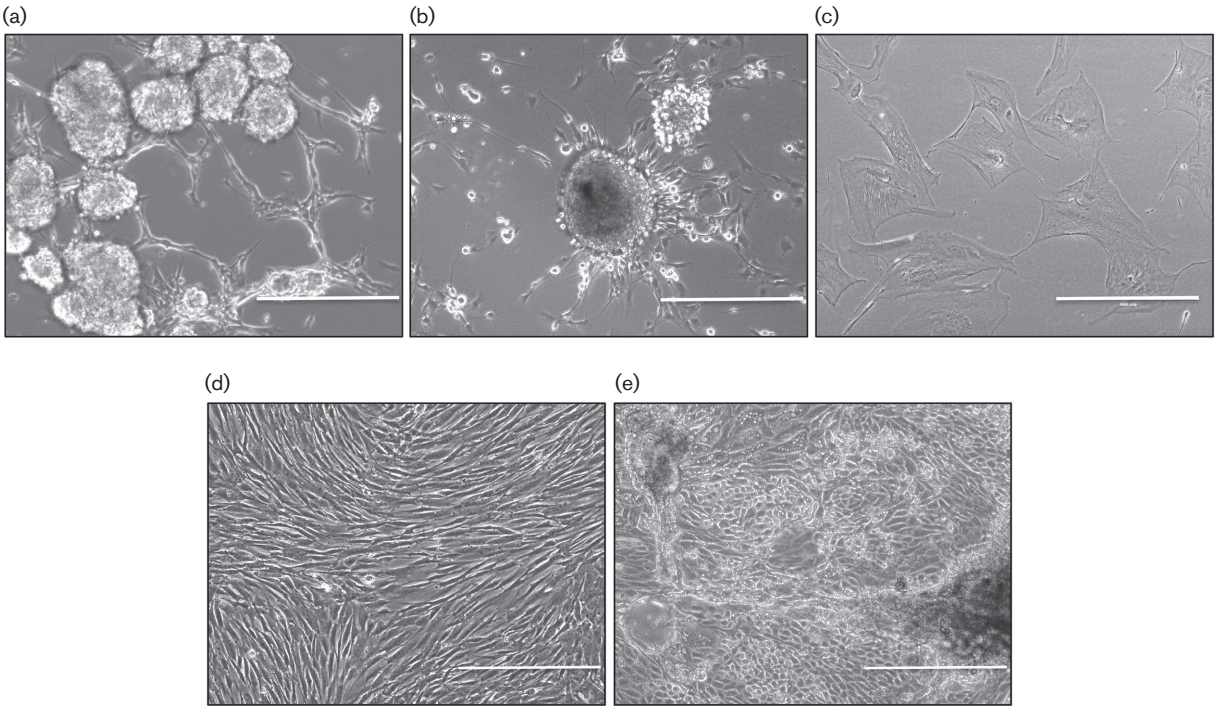

Fig. 1. Light microscopy images of primary cell culture demonstrating *in vitro* cytomorphology. (a) Neuroglial tumour cells (Rac14_0612 p6), (b) neural stem cells (Rac_1105 SVZ p0), (c) cortical astrocytes (Rac19_0822 Ctx p2), (d) dermal fibroblasts (Rac19_0822 Fibro p2), (e) renal tubular epithelium (PCRac_0716 p0). Scale bar, 400 μm.

marked reduction in the proportion of cells in S phase following treatment with JQ1 or IBET-151, with a shift in the majority of cells towards cell cycle arrest (G_1/G_0) (Figs 7a and S4). Cells treated with the inactive (−)-JQ1 demonstrated no such changes, and were identical to passage-matched control cells (Fig. S4).

We next sought a mechanism by which inhibition of BRD4 would result in loss of a stem cell state, increased differentiation, and cell cycle arrest. Given the role of BRD4 in gene transcription, we performed qRT-PCR with probes designed against the RacPyV T antigen and VP1 genes. We identified a significant decrease in viral gene transcription following inhibition of BRD4 with JQ1. Relative levels of both LT and VP1 were lower in JQ1-treated tumour cells compared with control tumour cells (Fig. 7b). JQ1-treated and control tumour cells were also analysed by qPCR in order to quantify the amount of viral genome present in the cells. Control tumour cells contained 6.2×10^4 viral equivalents per cell while cells treated with JQ1 contained 8.1×10^3 viral equivalents per cell, indicating a 7.65-fold loss of viral genome through inhibition of BRD4.

DISCUSSION

RacPyV is widely distributed throughout the body

We detected RacPyV DNA in every tissue examined, but found the highest quantities in tumour tissue relative to all other tissues. This wide tissue distribution and low viral quantity is consistent with persistent polyomaviral infections (Bialasiewicz *et al.*, 2009; Chesters *et al.*, 1983; Dubensky & Villarreal, 1984; Sadeghi *et al.*, 2014). Raccoon neuroglial brain tumour tissue contains high viral copies that are not associated with genetic mutation or insertion into the host cell genome (Dela Cruz *et al.*, 2013; Church *et al.*, 2016). This is in contrast to human polyomaviruses, in which disease-specific genotypes (JC polyomaviruses) or partial loss of viral genome associated with integration (Merkel cell polyomavirus) is identified (Gosert *et al.*, 2010; Feng *et al.*, 2008). Therefore, we propose properties unique to the neuroglial progenitor cell likely permit high viral replication and enables oncogenic transformation.

Tumour cell of origin is a neural stem cell

The consistent location of these tumours along the rostral migratory stream (RMS) within the olfactory tract led us to speculate that these tumours may arise from transformed neural progenitor/stem cells. Our *in vitro* culture of tumour cells demonstrate that these cells grow in an identical manner to neural stem cells, forming non-adherent neurospheres in a defined, serum-free medium. Most importantly, our immunocytochemistry and FACS results show that these tumour cells express markers associated with neural stem cell biology, namely CD133, sox2, olig2 and nestin, and co-express TuJ-1 and GFAP (Gage, 2000; Sanai *et al.*, 2005).

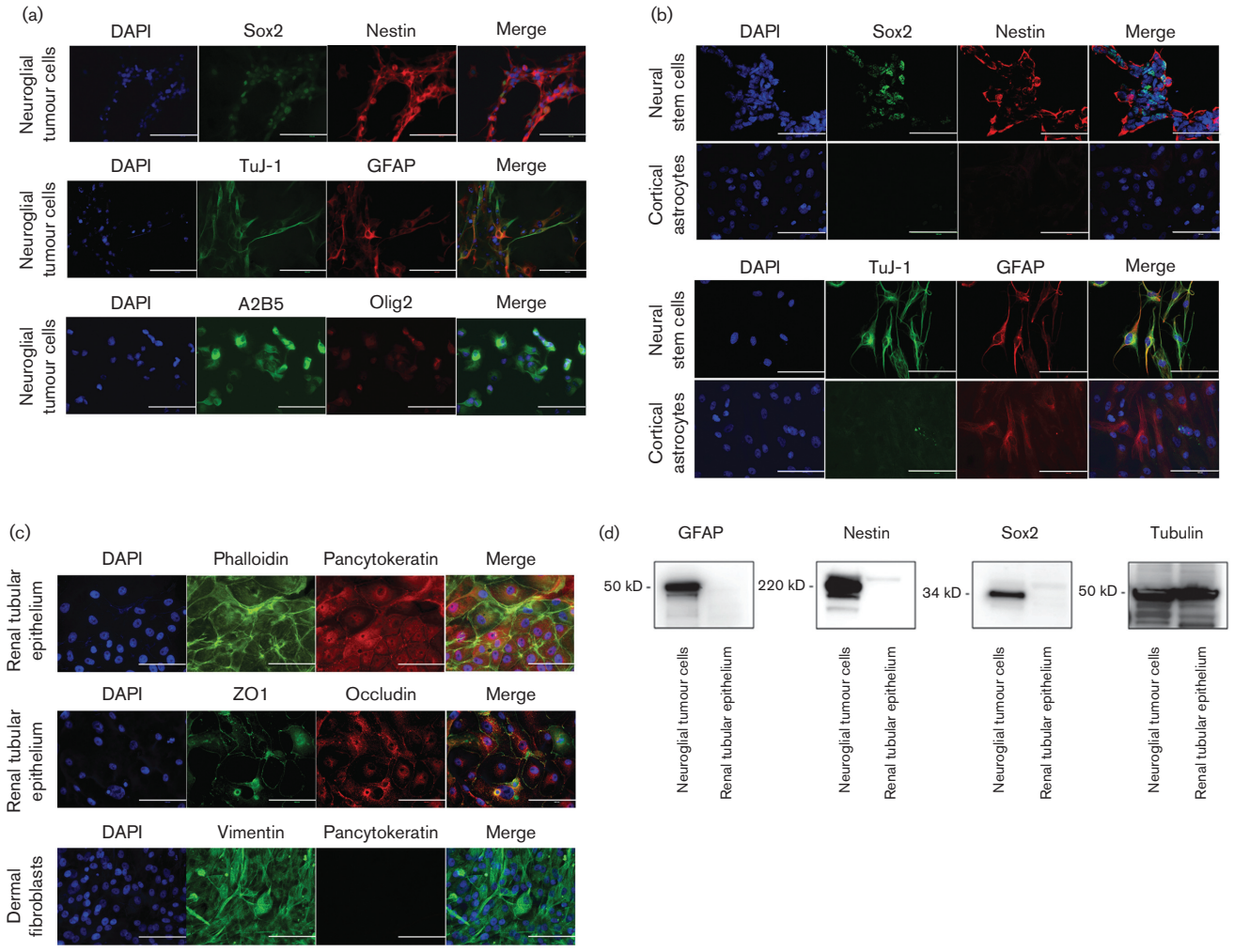

Fig. 2. (a, b, c) Immunocytochemistry characterization of primary cell lines. (a) Sox2, nestin, TuJ-1, GFAP, A2B5 and olig2 expression is present in neuroglial tumour cells. (b) Neural stem cells express sox2, nestin, TuJ-1 and GFAP. Cortical astrocytes express GFAP. (c) Actin (phalloidin stain), pancytokeratin, ZO1 and occludin expression in cultured renal tubular epithelium. Vimentin and pancytokeratin expression in cultured dermal fibroblasts. Bars, 100 μm (a–c). (d) Immunoblot of GFAP, nestin, sox2 and tubulin in primary cultures of tumour cells and renal tubular epithelium.

BRD4 is associated with RacPyV in neuroglial tumour cells

Prior studies (Brostoff *et al.*, 2014) established that RacPyV is maintained episomally through serial passages of tumour cell lines, which led us to investigate by what mechanism this occurs. The bromodomain-containing protein, BRD4, has been identified as a key protein involved in tethering DNA viruses, including Kaposi's sarcoma herpesvirus, Epstein–Barr virus, and human and bovine papillomaviruses, to host chromosomes in times of persistence (Lin *et al.*, 2008; You *et al.*, 2006; McBride & Jang, 2013; McBride *et al.*, 2012). BRD4 is also involved in DNA viral gene transcription and viral genome replication in papillomaviruses and Merkel cell polyomavirus (McBride & Jang, 2013; Ottinger *et al.*, 2006; Wang *et al.*, 2012). Recent work has also demonstrated a role for BRD4 in the maintenance of a pluripotent stem cell state, and in repressing differentiation in stem cells (Horne *et al.*, 2015; Wu *et al.*, 2015). Given this intersection, we investigated whether expression of BRD4 could account for the maintenance of RacPyV in neural stem cells and continued expression of oncogenic viral genes. It is of note that tumour tissue contains the highest detected levels of both BRD4 and RacPyV genome. Furthermore, our immunoprecipitation assay identifies an association between BRD4 and RacPyV. Given the chromatin-associated nature of BRD4, it is suggestive that BRD4 is physically tethered to the RacPyV genome, establishing a strong relationship between BRD4 and the viral genome. As BRD4 binds to acetylated chromatin domains, it is also involved in regulating gene transcription (Josling *et al.*, 2012; Mochizuki *et al.*, 2008). To examine whether BRD4 similarly regulates expression of RacPyV genes, we inhibited

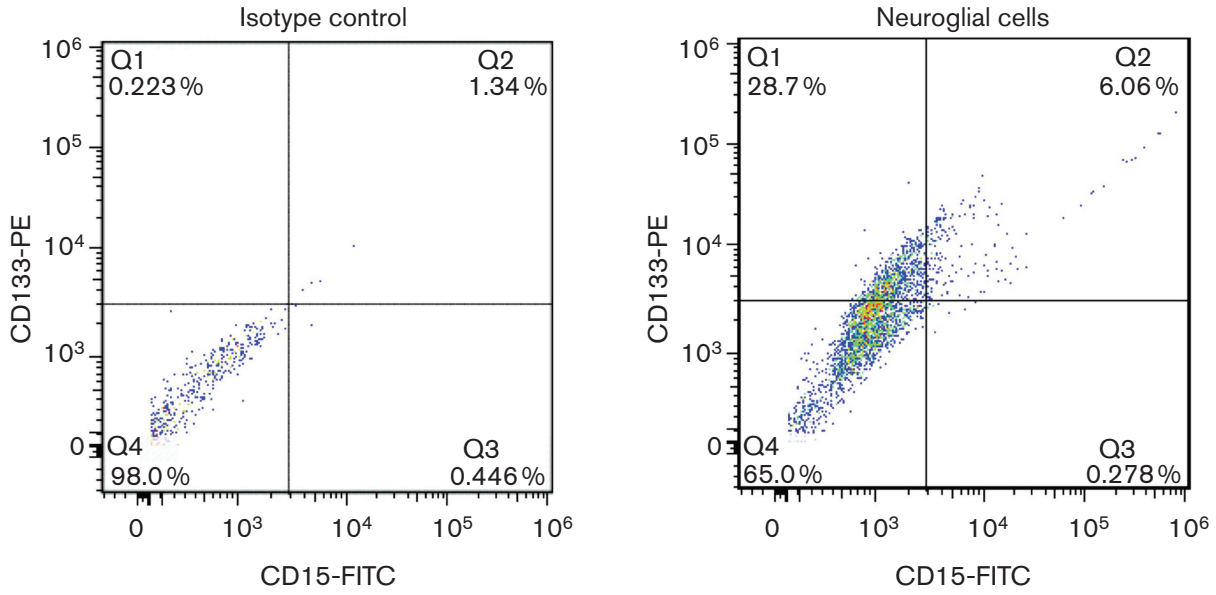

Fig. 3. Flow cytometry of neuroglial tumour cells stained with CD133 and CD15 shows CD133 expression in approximately 28 % of neuroglial cells. There is minimal CD15 expression.

BRD4 in tumour cells by treating them with the small molecule inhibitor, JQ1, which has been shown previously to inhibit BRD4. Inhibition of BRD4 in tumour cells results in a decreased viral copy number compared with the control, supporting the notion that BRD4 is specifically involved in physical maintenance of the viral genome in the host cell. The significant inhibition of expression in both early (LT) and late (VP1) genes indicates that BRD4 is involved not only in the physical maintenance of the viral genome, but also in regulating the expression of viral genes. Taken together, these data identify an important role for BRD4 in viral genome tethering, and in the regulation of viral gene expression.

BRD4 functions to maintain pluripotency in RacPyV tumour cells

Coinciding with inhibition of viral gene expression, JQ1 also significantly inhibits cellular proliferation. BRD4 inhibition rapidly shifts proliferating tumour cells to cell cycle arrest, and cells assume a more differentiated phenotype *in vitro*. Most interestingly, treatment of cells with JQ1 elicits a concomitant decrease in neural stem cell markers and an increase in markers of both neuronal and astroglial differentiation. To verify findings were attributable to BRD4 inhibition, cells were also treated with a second BET-inhibitor, IBET-151 (GSK1210151A), and the inactive JQ1 enantiomer, (−)-JQ1. A similar growth arrest and coincident increase in differentiation was identified following treatment with IBET-151, while the (−)-JQ1 showed no difference compared to control cells. Taken together, a role for BRD4 in the physical maintenance of RacPyV, regulation of viral gene expression, and maintenance of the neural stem cell state is defined in the context of neuroglial tumour formation by RacPyV.

Since BRD4 is expressed in a high quantity in neural stem cells, we believe that infection of these cells by RacPyV provides a unique microenvironment allowing for sustained expression of viral genes, ultimately favouring tumour formation. BRD4 plays an important role in the maintenance of stem cells (Di Micco *et al.*, 2014; Wu *et al.*, 2015), and we postulate that it is this stem cell state of the tumour cell of origin combined with oncogenic viral gene transcription that may explain why tumours are only present in the olfactory tract despite a systemic infection by RacPyV. Here, we have shown that BRD4 is important in transformation of

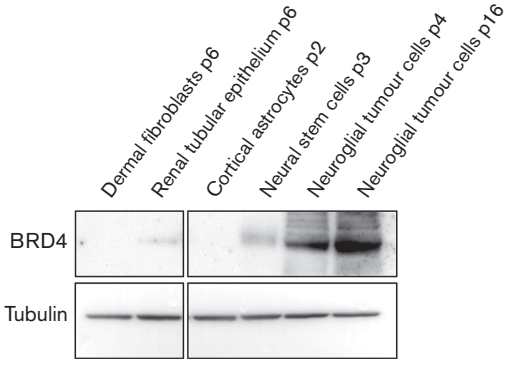

Fig. 4. Immunoblot of BRD4 expression in primary culture of different tissue types demonstrating highest expression in tumour cells, and relatively lower expression in neural stem cells. Minimal expression is noted in renal tubular epithelium.

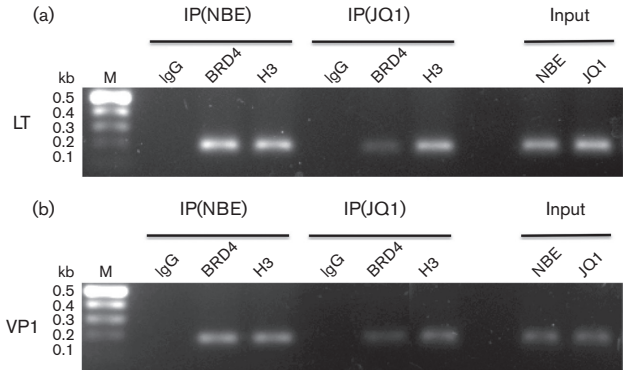

Fig. 5. Chromatin immunoprecipitation assay (ChIP) of cultured tumour cells control (NBE) and BRD4-inhibited (JQ1). Amount of RacPyV genome bound to BRD4 decreased with JQ1 treatment relative to control cells, as demonstrated by decrease in band intensity for (a) LT and (b) VP1.

tumour cells through both maintaining transcription of viral genes and by maintaining a stem cell state of the transformed cell by demonstrating that BRD4 (1) is associated with RacPyV genome, (2) mediates active RacPyV gene transcription, (3) is required for expression of neural stem cell markers, and (4) drives cell proliferation. These experiments further identify a growing role for BRD4 in viral genome maintenance and regulation of viral gene expression, and demonstrate for the first time its role in naturally occurring, viral oncogenic disease.

METHODS

Tissue distribution of RacPyV and quantitative PCR. In order to assess viral load in different tissues in raccoons, we collected tissues from raccoon carcasses in ordinance with a California Fish and Game scientific collecting permit (ID# 12154, Pesavento). A total of 121 raccoons from California were necropsied between 2010 and 2015. From those raccoons, 102 swabs of oropharyngeal and nasal mucosa, 96 faecal samples, 82 salivary glands, 78 urine samples, 52 brain samples, 33 skin/whisker samples, 27 lymphoid samples (including spleen, tonsil, lymph node and bone marrow), 22 kidney samples, 17 tumour samples and 14 spleen samples were analysed by quantitative real-time PCR (qPCR) for the presence of RacPyV genome.

Tissue samples were thawed in a chaotropic lysis buffer (DXB; Qiagen) and immediately homogenized in a GenoGrinder2000 (SpexCertiprep) for 2 min at 1000 strokes per minute. Homogenized tissue pieces were proteinase K-digested at 56 °C overnight. Total nucleic acids (including gDNA and RNA) were extracted from lysates with adapted standardized protocols as previously described (Mapes *et al.*, 2008). Briefly, lysates were extracted on Whatman filters in a Corbett X-Tractor platform (Qiagen). Nucleic acids were eluted into 150 µl PCR-grade nuclease-free

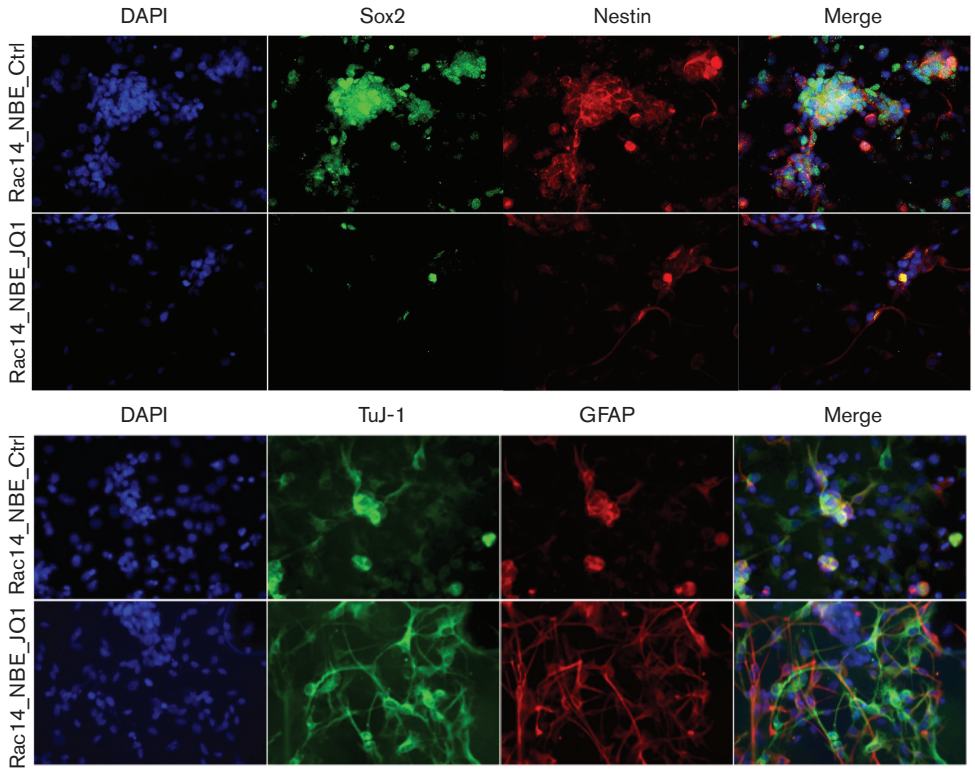

Fig. 6. Immunocytochemistry to measure expression of neuronal (TuJ-1) and glial (GFAP) markers in cultured tumour cells. Treatment with the BRD4 inhibitor JQ1 resulted in expression of either TuJ-1 or GFAP within individual cells and loss of co-expression of both markers within single cells, seen in the untreated tumour cells.

water (Fisher) and 5 µl aliquots were used in subsequent PCRs. Extracted DNA was then amplified by PCR using Taqman primers and probe designed to the VP1 gene (F primer: 5′-GTGATTTTAAAATATCTTGGTAAACCTCTG-3′, R primer: 5′-GCTATTTGTTTCCTGTGCAGACATC-3′ probe: 5′-CCATCCCCTCTGTCTTGTTGAAAAAACCAC-3′). We defined the threshold of positive to be 35 cycles or fewer. Many non-tumour samples exhibited cycle thresholds above 35, but displayed repeatable exponential amplification plots. Due to the high cycle threshold, we refer to these samples as minimally detectable.

Primary cell culture. Tissues were collected from raccoons humanely euthanized by licensed veterinarians as previously described (Brostoff *et al.*, 2014). Organs were aseptically dissected and placed into antibiotic-containing Dulbecco's modified Eagle's medium (DMEM)-F12

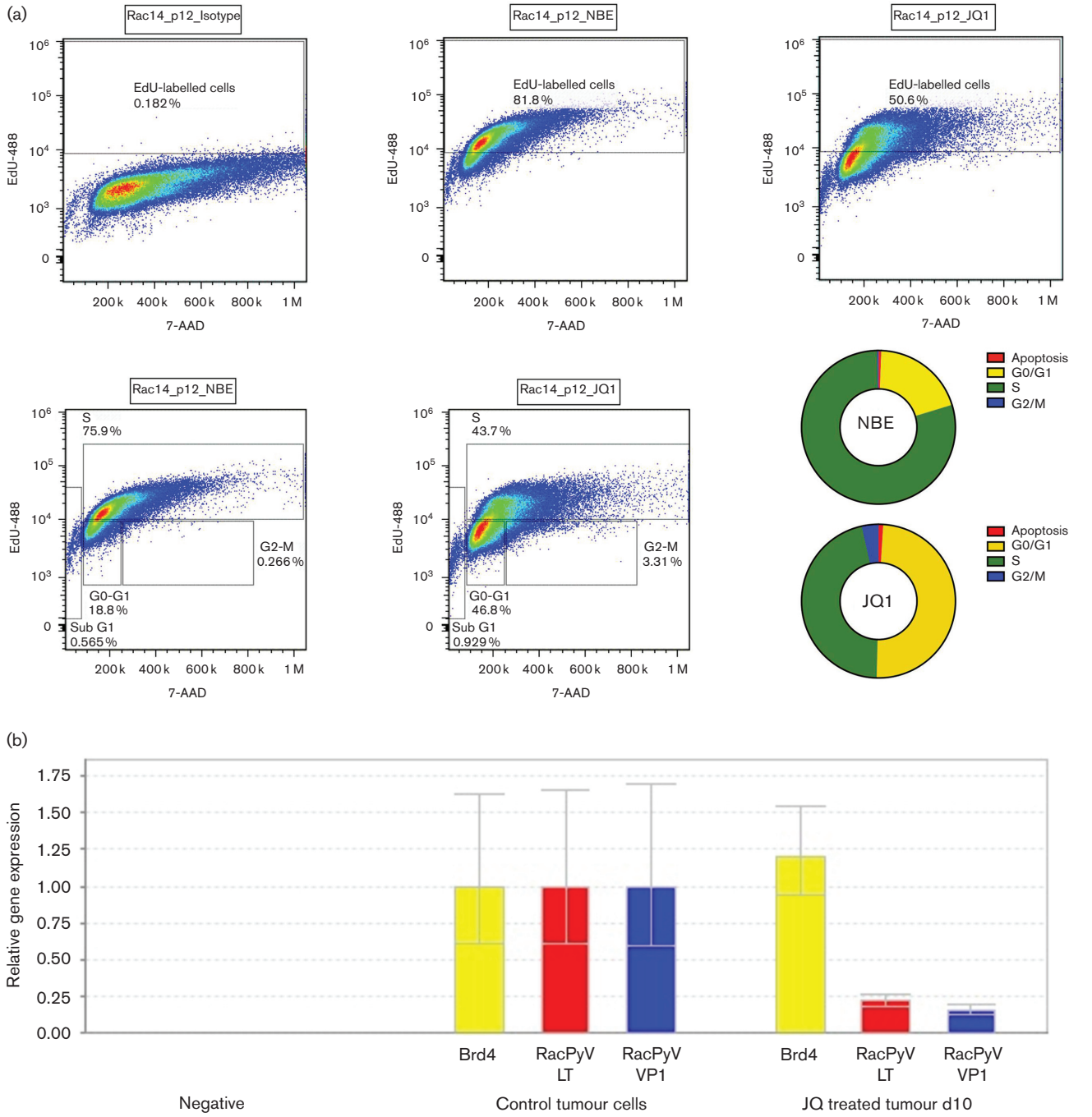

Fig. 7. (a) Cell cycle analysis by flow cytometry demonstrating a decrease in percentage of cells in S phase with inhibition of BRD4 by JQ1 treatment. (b) Real-time PCR assay for BRD4, Large T antigen (LT), and viral capsid protein (VP1) expression in control and JQ1-treated tumour cells. JQ1 treatment resulted in reduced expression of both LT and VP1. Error bars, standard deviation.

media and then minced by hand with scalpel blades. Tissues were mechanically triturated and resuspended in either 0.25 % trypsin (kidney-derived cells), 0.05 % trypsin (brain-derived cells), or 0.25 % trypsin plus 0.1 % collagenase (dermal fibroblasts), incubated at 37 °C for 3–5 min, and then further processed using a Miltenyi Biotec gentleMACS Tissue Dissociator. Tissue homogenate was then washed in PBS, resuspended in media and plated in T25 flasks (brain-derived tissue), gelatin-coated 10 cm tissue culture plates (kidney-derived cells), or uncoated 10 cm tissue culture plates (dermal fibroblasts) and maintained at 37 °C and 5 % CO_2.

Immunocytochemistry. Cells were plated onto laminin-coated cover glass at a count of 50 000 and grown to 80 % confluency, fixed in 4 % paraformaldehyde, blocked in 5 % normal goat serum in 0.2 % Triton PBS, and incubated overnight with primary antibodies at the following dilutions: sox2 (1 : 200, R&D Systems), nestin (1 : 200, Covance), TuJ-1 (1 : 500, Covance), GFAP (1 : 200, Dako), A2B5 (1 : 50, Zymed/Invitrogen), olig2 (1 : 100, Millipore), phalloidin (1 : 100, Life Technologies), cytokeratin AE1/AE3 (1 : 800, Dako), ZO1 (1 : 200, Abcam), occludin (1 : 500, ABfinity) and vimentin (1 : 1000, Novus). Cells were then washed and incubated with fluorochrome-conjugated anti-mouse and anti-rabbit (Life Technologies) antibodies at a dilution of 1 : 1000. Cells were then stained with DAPI (1 mg ml^{-1} in PBS, ThermoFisher) and washed. Finally, cover glass were mounted onto microscope slides using VECTASHIELD HardSet Antifade Mounting Medium (Vector Laboratories).

Fluorescence-activated cell sorting. Tumour cells were grown to confluency, trypsinized, washed with FACS buffer and fixed with 4 % paraformaldehyde. Cells were then incubated with mouse monoclonal anti-CD15 IgM antibody (1 : 100 dilution, BD) and rabbit polyclonal anti-CD133 IgG antibody (1 : 10 dilution, Santa Cruz Biotechnology) for 10 min at 4 °C. Cells were washed and incubated with secondary antibody conjugated to FITC (CD15) and PE (CD133) in the dark at room temperature for 30 min, and then were washed and stained with 7AAD prior to analysis. Cells were analysed on a Beckman Coulter FC-500 flow cytometer and gated according to matched isotype controls. Analysis of subpopulations was performed using FlowJo software.

Viral and host gene expression. In order to assess viral and host gene expression, a real-time reverse transcriptase PCR assay was developed and applied as previously described (Brostoff *et al.*, 2014). Primers and probes were designed for VP1 from a consensus RacPyV sequence and for BRD4-utilizing sequence analysis from transcriptome results (Brostoff *et al.*, 2014).

Immunoblotting. Immunoblotting was performed by lysing cell pellets in commercial lysis buffer (RIPA; ThermoScientific) followed by sonication (Active Motif). Protein was quantified and 20 µg was loaded into each well and then electrophoresed through a 4–12 % Bis/Tris polyacrylamide gel (Life Technologies) before being transferred to a PVDF membrane. Membranes were blocked in 5 % milk in Tris-buffered saline and 0.05 % Tween 20 (TBST) solution, and primary antibodies were incubated with rabbit monoclonal anti-BRD4 antibody (Cell Signaling) at a dilution of 1 : 1000 in 5 % BSA/TBST. Membranes were then incubated with HRP-conjugated anti-rabbit antibody at 1 : 10 000 (ThermoFisher), washed in TBST, and developed with Amersham ECL (GE Life Sciences).

Chromatin immunoprecipitation. Chromatin immunoprecipitation (ChIP) was performed using SimpleChIP Plus Enzymatic Chromatin IP Kit with Magnetic Beads (Cell Signaling) following the manufacturer's protocol. Briefly, tumour cells were grown to approximately 80 % confluence on 15 cm plates in 20 ml media. Cells were incubated at room temperature for 10 min with 37 % formaldehyde, followed by a 5 min incubation with glycine, and were then scraped into ice-cold PBS and collected. Cell pellets were then lysed in protease inhibitor, micrococcal nuclease was added to digest DNA, and mixtures were sonicated to lyse nuclei. Digested chromatin was subsequently incubated with antibodies to BRD4 (Cell Signaling), Histone H3 (Cell Signaling) or Rabbit IgG (Cell Signaling). Following immunoprecipitation in a magnetic column, nucleic acid was eluted and PCR performed using primers specific to either LT (Fwd: 5′-TTTCGGATTCTCCAGTCAGACATCGA-3′, Rev: 5′-TTGGAGGTGTGCTTGAGAAACTTCCTC-3′) or VP1 (Fwd: 5′-TGCACATGAATATGAAGGAAGGTGCTC-3′, Rev: 5′-ATTGTGA CAGGCCCTGATAGTATAACTGAAATAG-3′) of RacPyV. PCR products were electrophoresed on an agarose gel and imaged.

BRD4 inhibition. Rac14_0612 tumour cells were cultured in serum-free media as previously reported (Brostoff *et al.*, 2014). Cells were treated with either JQ1 (Tocris Bioscience) dissolved in ethanol to a final concentration of 250 nM, IBET-151 (GSK1210151A) at a concentration of 1 µM, the inactive (−)-JQ1 at 250 nM, or matched volumes of ethanol alone. Media containing JQ1, IBET-151, or ethanol was changed daily for 3 days before cells were collected.

Quantitative real-time reverse transcriptase PCR. RNA was extracted from cell pellets (RNeasy kit; Qiagen) and all samples were treated with on-column DNase (Qiagen) prior to cDNA conversion to eliminate any genomic DNA, and RNA was reverse transcribed with ABI High Capacity RNA to cDNA conversion kit (Applied Biosystems). cDNA was assayed in triplicate with primer sets and Taqman probes were designed against target sequences in LT, VP1 and BRD4 (Table S1). Sequence data for each gene was mined from RNA-sequencing as previously published (Brostoff *et al.*, 2014). For LT and BRD4, primer sets were aligned to adjoining exons, with a Taqman probe spanning the exon–exon junction.

MTT assay. To evaluate cell proliferation, Rac14_0612 cells were cultured either in NBE or NBE+JQ1 for 3 days at an identical concentration to above (250 nM). Briefly, cells were seeded into 96-well plates at an initial concentration of 5×10^4 cm^{-1} and then either maintained in NBE or treated with JQ1 for 3 days, after which cells were incubated with 3-[4,5-dimethylthiazol-2-yl]-2,5-diphenyl tetrazolium bromide (MTT, Sigma Aldrich) at an amount equal to 10 % of culture medium volume for 2 h at 37 °C. Solubilization solution (100 µl) was added and gently mixed. Plates were then read on a spectrophotometer at a wavelength of 570 nm (Molecular Devices).

Cell cycle analysis. Rac14_0612 tumour cells were cultured in either NBE, NBE+JQ1, NBE+ (−)-JQ1, or NBE+IBET-151 for 3 days, at concentrations reported above. Following this treatment, cells were labelled with EdU according to the manufacturer's recommendations (Life Technologies). Briefly, cells were incubated with 10 µM EdU for 2 h at 37 °C before being fixed, permeabilized and labelled with the DNA stain 7-AAD. Cells were analysed on a Beckman Coulter FC-500 flow cytometer and gated according to EdU uptake and DNA content. Analysis of subpopulations was performed using FloJo software.

REFERENCES

Ahmed, S. (2009). The culture of neural stem cells. *J Cell Biochem* **106**, 1–6.

Bialasiewicz, S., Whiley, D. M., Lambert, S. B., Nissen, M. D. & Sloots, T. P. (2009). Detection of BK, JC, WU, or KI polyomaviruses in faecal, urine, blood, cerebrospinal fluid and respiratory samples. *J Clin Virol* **45**, 249–254.

Brostoff, T., Dela Cruz, F. N., Church, M. E., Woolard, K. D. & Pesavento, P. A. (2014). The raccoon polyomavirus genome and tumor antigen transcription are stable and abundant in neuroglial tumors. *J Virol* **88**, 12816–12824.

Chesters, P. M., Heritage, J. & McCance, D. J. (1983). Persistence of DNA sequences of BK virus and JC virus in normal human tissues and in diseased tissues. *J Infect Dis* **147**, 676–684.

Church, M. E., Dela Cruz, F. N., Estrada, M., Leutenegger, C. M., Pesavento, P. A. & Woolard, K. D. (2016). Exposure to raccoon polyomavirus (RacPyV) in free-ranging North American raccoons (*Procyon lotor*). *Virology* **489**, 292–299.

DeCaprio, J. A. & Garcea, R. L. (2013). A cornucopia of human polyomaviruses. *Nat Rev Microbiol* **11**, 264–276.

Dela Cruz, F. N., Giannitti, F., Li, L., Woods, L. W., Del Valle, L., Delwart, E. & Pesavento, P. A. (2013). Novel polyomavirus associated with brain tumors in free-ranging raccoons, western United States. *Emerg Infect Dis* **19**, 77–84.

Di Micco, R., Fontanals-Cirera, B., Low, V., Ntziachristos, P., Yuen, S. K., Lovell, C. D., Dolgalev, I., Yonekubo, Y., Zhang, G. & other authors (2014). Control of embryonic stem cell identity by BRD4-dependent transcriptional elongation of super-enhancer-associated pluripotency genes. *Cell Rep* **9**, 234–247.

Dubensky, T. W. & Villarreal, L. P. (1984). The primary site of replication alters the eventual site of persistent infection by polyomavirus in mice. *J Virol* **50**, 541–546.

Feng, H., Shuda, M., Chang, Y. & Moore, P. S. (2008). Clonal integration of a polyomavirus in human Merkel cell carcinoma. *Science* **319**, 1096–1100.

Ferenczy, M. W., Johnson, K. R., Marshall, L. J., Monaco, M. C. & Major, E. O. (2013). Differentiation of human fetal multipotential neural progenitor cells to astrocytes reveals susceptibility factors for JC virus. *J Virol* **87**, 6221–6231.

Gage, F. H. (2000). Mammalian neural stem cells. *Science* **287**, 1433–1438.

Giannitti, F., Higgins, R. J., Pesavento, P. A., Dela Cruz, F., Clifford, D. L., Piazza, M., Parker Struckhoff, A., Del Valle, L., Bollen, A. W. & other authors (2014). Temporal and geographic clustering of polyomavirus-associated olfactory tumors in 10 free-ranging raccoons (*Procyon lotor*). *Vet Pathol* **51**, 832–845.

Gosert, R., Kardas, P., Major, E. O. & Hirsch, H. H. (2010). Rearranged JC virus noncoding control regions found in progressive multifocal leukoencephalopathy patient samples increase virus early gene expression and replication rate. *J Virol* **84**, 10448–10456.

Horne, G. A., Stewart, H. J., Dickson, J., Knapp, S., Ramsahoye, B. & Chevassut, T. (2015). Nanog requires BRD4 to maintain murine embryonic stem cell pluripotency and is suppressed by bromodomain inhibitor JQ1 together with Lefty1. *Stem Cells Dev* **24**, 879–891.

Josling, G. A., Selvarajah, S. A., Petter, M. & Duffy, M. F. (2012). The role of bromodomain proteins in regulating gene expression. *Genes* **3**, 320–343.

Lemasson, G., Coquart, N., Lebonvallet, N., Boulais, N., Galibert, M. D., Marcorelles, P. & Misery, L. (2012). Presence of putative stem cells in Merkel cell carcinomas. *J Eur Acad Dermatol Venereol* **26**, 789–795.

Lin, A., Wang, S., Nguyen, T., Shire, K. & Frappier, L. (2008). The EBNA1 protein of Epstein-Barr virus functionally interacts with Brd4. *J Virol* **82**, 12009–12019.

Liu, W., Stein, P., Cheng, X., Yang, W., Shao, N. Y., Morrisey, E. E., Schultz, R. M. & You, J. (2014). BRD4 regulates Nanog expression in mouse embryonic stem cells and preimplantation embryos. *Cell Death Differ* **21**, 1950–1960.

Mapes, S., Leutenegger, C. M. & Pusterla, N. (2008). Nucleic acid extraction methods for detection of EHV-1 from blood and nasopharyngeal secretions. *Vet Rec* **162**, 857–859.

McBride, A. A., Sakakibara, N., Stepp, W. H. & Jang, M. K. (2012). Hitchhiking on host chromatin: how papillomaviruses persist. *Biochim Biophys Acta* **1819**, 820–825.

McBride, A. A. & Jang, M. K. (2013). Current understanding of the role of the Brd4 protein in the papillomavirus lifecycle. *Viruses* **5**, 1374–1394.

Mochizuki, K., Nishiyama, A., Jang, M. K., Dey, A., Ghosh, A., Tamura, T., Natsume, H., Yao, H. & Ozato, K. (2008). The bromodomain protein Brd4 stimulates G1 gene transcription and promotes progression to S phase. *J Biol Chem* **283**, 9040–9048.

Moore, P. S. & Chang, Y. (2010). Why do viruses cause cancer? Highlights of the first century of human tumour virology. *Nat Rev Cancer* **10**, 878–889.

Ottinger, M., Christalla, T., Nathan, K., Brinkmann, M. M., Viejo-Borbolla, A. & Schulz, T. F. (2006). Kaposi's sarcoma-associated herpesvirus LANA-1 interacts with the short variant of BRD4 and releases cells from a BRD4- and BRD2/RING3-induced G1 cell cycle arrest. *J Virol* **80**, 10772–10786.

Reynolds, B. A. & Weiss, S. (1992). Generation of neurons and astrocytes from isolated cells of the adult mammalian central nervous system. *Science* **255**, 1707–1710.

Rodriguez, R. M., Suarez-Alvarez, B., Salvanés, R., Huidobro, C., Toraño, E. G., Garcia-Perez, J. L., Lopez-Larrea, C., Fernandez, A. F., Bueno, C. & other authors (2014). Role of BRD4 in hematopoietic differentiation of embryonic stem cells. *Epigenetics* **9**, 566–578.

Sadeghi, M., Aaltonen, L. M., Hedman, L., Chen, T., Söderlund-Venermo, M. & Hedman, K. (2014). Detection of TS polyomavirus DNA in tonsillar tissues of children and adults: evidence for site of viral latency. *J Clin Virol* **59**, 55–58.

Sanai, N., Alvarez-Buylla, A. & Berger, M. S. (2005). Mechanisms of disease: neural stem cells and the origin of gliomas. *N Engl J Med* **353**, 811–822.

Sun, W., Kim, H. & Moon, Y. (2010). Control of neuronal migration through rostral migration stream in mice. *Anat Cell Biol* **43**, 269–279.

Swanson, P. A., Lukacher, A. E. & Szomolanyi-Tsuda, E. (2009). Immunity to polyomavirus infection: the polyomavirus–mouse model. *Semin Cancer Biol* **19**, 244–251.

Tilling, T. & Moll, I. (2012). Which are the cells of origin in Merkel cell carcinoma? *J Skin Cancer* **2012**, 680410.

Wang, X., Li, J., Schowalter, R. M., Jiao, J., Buck, C. B. & You, J. (2012). Bromodomain protein Brd4 plays a key role in Merkel cell polyomavirus DNA replication. *PLoS Pathog* **8**, e1003021.

White, M. K., Gordon, J. & Khalili, K. (2013). The rapidly expanding family of human polyomaviruses: recent developments in understanding their life cycle and role in human pathology. *PLoS Pathog* **9**, e1003206.

Wirth, J. J., Martin, L. G. & Fluck, M. M. (1997). Oncogenesis of mammary glands, skin, and bones by polyomavirus correlates with viral persistence and prolonged genome replication potential. *J Virol* **71**, 1072–1078.

Wollebo, H. S., Bellizzi, A., Cossari, D. H., Salkind, J., Safak, M. & White, M. K. (2016).). The Brd4 acetyllysine-binding protein is involved in activation of polyomavirus JC. *J Neurovirol* **22**, 615–625.

Wu, T., Pinto, H. B., Kamikawa, Y. F. & Donohoe, M. E. (2015). The BET family member BRD4 interacts with OCT4 and regulates pluripotency gene expression. *Stem Cell Reports* **4**, 390–403.

You, J., Croyle, J. L., Nishimura, A., Ozato, K. & Howley, P. M. (2004). Interaction of the bovine papillomavirus E2 protein with Brd4 tethers the viral DNA to host mitotic chromosomes. *Cell* **117**, 349–360.

You, J., Srinivasan, V., Denis, G. V., Harrington, W. J., Ballestas, M. E., Kaye, K. M. & Howley, P. M. (2006). Kaposi's sarcoma-associated herpesvirus latency-associated nuclear antigen interacts with bromodomain protein Brd4 on host mitotic chromosomes. *J Virol* **80**, 8909–8919.